Oxidative stress in experimental bronchopulmonary dysplasia

Horst, S.A.J. ter

Chapter

5

Inhaled nitric oxide attenuates pulmonary inflammation and fibrin deposition and prolongs survival in neonatal hyperoxic lung injury

Inhaled nitric oxide attenuates pulmonary inflammation and fibrin deposition and prolongs survival in neonatal hyperoxic lung injury

Simone A.J. ter Horst
Frans J. Walther
Ben J.H.M. Poorthuis
Pieter S. Hiemstra
Gerry T.M. Wagenaar

Am J Physiol Lung Cell Moll Physiol 293(1):L35-L44, 2007

ABSTRACT

Administration of inhaled nitric oxide (iNO) is a potential therapeutic strategy to prevent bronchopulmonary dysplasia (BPD) in preterm newborns with respiratory distress syndrome. We evaluated this approach in a rat model, in which preterm pups were exposed to room air, hyperoxia or a combination of hyperoxia and NO (8.5 and 17 ppm). We investigated the anti-inflammatory effects of prolonged iNO therapy by studying survival, histopathology, fibrin deposition, and differential mRNA expression (*real-time* RT-PCR) of key genes involved in the development of BPD. iNO therapy prolonged median survival 1.5 days (p = 0.0003), reduced fibrin deposition in a dosage dependent way up to 4.3-fold (p < 0.001), improved alveolar development by reducing septal thickness, and reduced the influx of leukocytes. Analysis of mRNA expression revealed an iNO-induced downregulation of genes involved in inflammation (IL-6, cytokine-induced neutrophilic chemoattractant-1 and amphiregulin), coagulation and fibrinolysis (plasminogen activator inhibitor 1 and urokinase-type plasminogen activator receptor), cell-cycle regulation (p21), and an upregulation of fibroblast growth factor receptor-4 (alveolar formation). We conclude that iNO therapy improves lung pathology and prolongs survival by reducing septum thickness, inhibiting inflammation, and reducing alveolar fibrin deposition in preterm rat pups with neonatal hyperoxic lung injury.

Key words: oxidative stress, Bronchopulmonary dysplasia, premature rats, coagulation, fibrinolysis.

INTRODUCTION

Pharmacological and technical advances in neonatal intensive care medicine have greatly improved survival and morbidity of premature infants. However, premature infants with respiratory distress syndrome (RDS) are very susceptible to develop bronchopulmonary dysplasia (BPD) as a result of oxygen therapy, mechanical ventilation and surfactant deficiency, especially when they are born at <30 wk of gestation and a birth weight of <1,200 g (19). Premature infants suffering from BPD have a chronic lung disease that requires oxygen therapy at 36 wk of gestation. BPD is characterized by an arrest in alveolar and vascular lung development, inflammation, and abnormal coagulation and fibrinolysis resulting in alveolar fibrin deposition and oxidative stress (19) and can be complicated by pulmonary hypertension (10).

Administration of inhaled nitric oxide (iNO) is a potential novel therapeutic strategy for premature infants with RDS who are at risk to develop BPD. In the mammalian lung, three NO synthases neuronal (nNOS), inducible (iNOS) and endothelial (eNOS)] synthesize equimolar amounts of NO and L-citrullin from L-arginine and oxygen (8, 34). In the airways, NOS is present in many cell types, including vascular endothelial cells, airway epithelial cells, macrophages and neurons. NO is a gas that exerts its biological function in part via the activation of guanylate cyclase, resulting in the production of cGMP (20). NO is involved in multiple (patho)physiological processes in the lung, including neurotransmission, pulmonary circulation, smooth muscle contraction, inflammatory mechanisms, ciliary motility, mucin secretion and plasma exudation (1, 6, 8, 20, 25).

Persistent pulmonary hypertension of the newborn is a common complication in full-term infants with respiratory failure and can be alleviated by administration of iNO (5, 38), which induces vasodilatation, improves oxygenation (5, 38), reduces the need for extracorporeal membrane oxygenation (5), and shortens the stay in the neonatal intensive care unit (38). Although preterm infants with severe RDS often develop pulmonary hypertension (42), the use of low dosages of iNO (5-10 ppm) to prevent BPD is still controversial (2, 14, 22, 23, 29), as only a limited number of clinical trial has reported a decrease in the incidence of both BPD and death (23, 33).

iNO exerts beneficial effects on acute hyperoxic lung injury in adult rats by attenuating endothelial and alveolar epithelial cell injury (28), free radical mediated effects (39), inflammation and apoptosis (16), and prolonging survival (12, 30), and on endotoxic lung injury by reducing procoagulant activity (20). Although iNO improves alveolarization (25) and pulmonary function and decreases elastin deposition (27) and surfactant inactivation (18) in animal models of BPD, the mechanism by which iNO improves hyperoxia-induced lung injury at clinically relevant dosages is still unclear. Therefore, we first investigated the effects of prolonged exposure to 8.5 and 17 ppm of iNO for 10 days on fibrin deposition (Western blotting) and differential mRNA expression of key genes of pathways involved in the

development of BPD (41) in premature rat pups with hyperoxia-induced lung injury, to determine the optimal NO concentration. Since 17 ppm iNO showed the most significant beneficial effects in experimental BPD on fibrin deposition and differential mRNA expression, we studied the effects of 17 ppm iNO exposure on survival, protein leakage and quantitative histochemistry in our animal model for BPD.

MATERIALS AND METHODS

Animals. Timed-pregnant Wistar rats were kept in a 12 h dark/light cycle and fed a standard chow diet (Special Diet Services; Witham, Essex, UK) ad libitum. Breeding pairs were allowed access for 1 hour at the day female Wistar rats showed very specific sexual behaviour, such as lordosis, hopping and air-flapping. After a gestation of ~21.5 days, pregnant Wistar rats were killed by decapitation (spontaneous birth occurs 22 days after conception), and pups were delivered by hysterectomy through a median abdominal incision to ensure that the delay in birth between the first and the last pup was only 5 min. Immediately after birth, pups were dried and stimulated. Pups from four litters were pooled and distributed over two experimental groups, i.e., an oxygen (O_2) and an oxygen/nitric oxide (NO) group, and room air-exposed (RA) control groups. Litter size was 12 pups per litter in the experimental groups. Pups were kept in a transparent 50 x 50 x 70-cm Plexiglas chamber for 10 days or until death occurred (survival experiments). In this way, influences of the birth process within and between litters could be avoided, and exposure to hyperoxia and NO could be started within 30 min after birth. Pups were fed by lactating foster dams, which were rotated daily to avoid oxygen toxicity. Foster dams were exposed to 100% oxygen for 24 h at 72-h intervals and to room air for 48 h. The oxygen concentration was kept at 100% using a flow of 5 l/min. In a pilot experiment in which rats were exposed to 10 or 20 ppm NO under hyperoxia, we found a remarkable reduction in fibrin deposition, our most sensitive parameter for lung tissue damage, with 20 ppm NO. At up to 17 ppm NO, the NO_2 concentration remained less than 2.5 ppm, and potential harmful effects of NO_2, i.e., generation of met-hemoglobin, could be prevented. Therefore, we initially treated rats with 17 ppm NO. To demonstrate a concentration-dependent effect of NO-treatment in experimental BPD, we also studied the effect of 8.5 ppm NO, which is within the range of 5-10 ppm used clinically, on fibrin deposition and mRNA expression. The NO concentration was kept at 8.5 ppm using a NO flow of 0.058 l/min or 17 ppm using a NO flow of 0.122 l/min (Del NO 1,000 adjustable NO flow pump, Sensormedics). Oxygen, NO and NO_2 concentrations were monitored twice a day with an oxygen sensor (Drägerwerk, Lübeck, Germany) and a NO-NO_2 sensor (Sensormedics). Weight, evidence of disease, and mortality were also checked twice a day. The research protocol was approved by the Institutional Animal Care and

Use Committee of the Leiden University Medical Center.

Tissue preparation. Pups were anesthetized with an intraperitoneal injection of ketamine (50 mg/kg body wt; Nimatek, Eurovet Animal Health, Bladel, The Netherlands) and xylazine (50 mg/kg bodyweight; Rompun, Bayer, Leverkusen, Germany). To avoid postmortem fibrin deposition in the lungs, heparin (100 units; Leo Pharma, Breda, The Netherlands) was injected intraperitoneally. After 5 min, pups were exsanguinated by transection of the abdominal blood vessels. The thoracic cavity was opened, and the lungs were removed, snap-frozen in liquid nitrogen, and stored at –80°C until use for real-time RT-PCR or the fibrin deposition assay. For histology studies, the trachea was cannulated (Bioflow 0.6-mm intravenous catheter; Vygon, Veenendaal, The Netherlands), and the lungs were fixed in situ via the trachea cannula with buffered formaldehyde (4% paraformaldehyde in PBS, pH 7.4) at 25 cmH_2O pressure for 3 min. Lungs were removed, fixed additionally in formaldehyde for 24 h at 4°C, and embedded in paraffin after dehydration in a graded alcohol series and xylene.

Bronchoalveolar lavages. Pups were anesthetized with an intraperitoneal injection of ketamine and xylazine and injected intraperitoneally with heparin. A cannula (Bioflow 0.6-mm intravenous catheter) was positioned in the trachea, and the pups were exsanguinated by transection of the abdominal blood vessels. Lungs were slowly lavaged four times with 500 μl of 0.15 M NaCl, 1 mM EDTA (pH 8.0), without opening the thorax. Samples were pooled, stored temporarely at 4°C, and centrifuged for 10 min at 5,000 rpm. Supernatants were stored at -20°C until further use.

Lung histology. Lung paraffin sections (5 μm) were cut and mounted onto SuperFrost plus-coated slides (Menzel, Braunschweig, Germany). After deparaffinization, sections were stained with hematoxylin and eosin, with a monoclonal anti-human fibrin antibody (59D8) that specifically recognizes the β-chain of fibrin (17, 41) or with monoclonal ED-1 that specifically recognizes rat monocytes and macrophages (7). For immunohistochemistry, sections were incubated with 0.3% H_2O_2 in methanol to block endogenous peroxidase activity. After a graded alcohol series, sections were boiled in 0.01 M sodium citrate (pH 6.0) for 10 min. Sections were incubated overnight with 59D8 or ED-1, stained with EnVision-HRP (Dako, Glostrup, Denmark), using NovaRed (Vector, Burlingame, CA) as chromogenic substrate, and counterstained briefly with hematoxylin or nuclear fast red. For morphometry, an eye piece reticle with a coherent system of 21 lines and 42 points (Weibel type II ocular micrometer; Paes, Zoeterwoude, The Netherlands) was used. Mean linear intercept (Lm), an indicator of mean alveolar diameter, and alveolar surface area were assessed in 10 nonoverlapping fields (surface area per field: 0.28 mm^2) in one representative section for each animal at a X200 magnification (26). Alveolar surface area was expressed as mm^2 per field. The density of ED-1 positive monocytes and macrophages was determined by counting the number of cells per field. Fields containing large blood vessels or bronchioli were excluded from the analysis. Results were expressed as cells/mm^2. Per

experimental animal, 22 fields in one section were studied at a X400 magnification. At least 6 different rat pups per experimental group were studied.

Fibrin detection assay. Fibrin deposition in lungs was detected as described previously (41). Briefly, frozen lungs were homogenized with an Ultra-Turrax T25 basic tissue homogenizer (IKA-Werke, Staufen, Germany) for 1 min at full speed in a cold 10 mM sodium phosphate buffer (pH 7.5), containing 5 mM EDTA, 100 mM ε-aminocaproic acid, 10 U/ml aprotinin, 10 U/ml heparin, and 2 mM PMSF. The homogenate was incubated for 16 h on a top-over-top rotor at 4°C. After centrifugation (10,000 rpm, 4°C, 10 min), the pellet was resuspended in extraction buffer [10 mM sodium phosphate buffer (pH 7.5), 5 mM EDTA, and 100 mM ε-aminocaproic acid] and recentrifuged. Pellets were suspended in 3 M urea, extracted for 2 h at 37°C, and centrifuged at 14,000 rpm for 15 min. After the supernatant was aspirated and discarded, the pellet was dissolved at 65°C in reducing sample buffer (10 mM Tris, pH 7.5, 2% SDS, 5% glycerol, 5% β-mercaptoethanol, and 0.4 mg/ml bromophenol blue) for 90 min with vortexing every 15 min. Hereafter, samples were subjected to SDS-PAGE (7.5%; 5% stacking) and blotted onto PVDF membrane (Immobilon-P, Millipore). The 56-kDa fibrin β-chains were detected with monoclonal 59D8, which specifically recognizes β-fibrin (17, 41), using ECL plus Western blotting detection system and Hyperfilm ECL (Amersham Biosciences, Arlington Heights, IL). Exposures were quantified with a Bio-Rad GS-800 calibrated densitometer using the Quantity One version 4.4.1 software package (Bio-Rad, Veenendaal, the Netherlands). Fibrin deposition was quantified in lungs of at least 10 rats/experimental group. As a reference, fibrin standards were generated from rat fibrinogen (Sigma, St. Louis, MO). After rat fibrinogen was solubilized in two-thirds strength PBS (pH 7.4), human α-thrombin (Sigma) was added, vortexed, and incubated at 37°C for 10 min. After addition of 2X SDS sample buffer, the fibrin sample was vortexed and incubated at 65°C for 90 min; aliquots were frozen at −80°C until use.

Real-time RT-PCR. Total RNA was isolated from lung tissue homogenates using guanidium-phenol extraction (RNA-Bee; Tel-Test, Bio-Connect, Huissen, The Netherlands). Briefly, after tissue homogenization in RNA-Bee, RNA was isolated using phenol-chloroform extraction and isopropanol precipitation. The RNA sample was dissolved in RNase-free water and quantified spectrophotometrically. The integrity of the RNA was studied by gel electrophoresis on a 1% agarose gel, containing ethidium bromide. Samples did not show degradation of ribosomal RNA by visual inspection under ultraviolet light. First-strand cDNA synthesis was performed with the SuperScript Choice System (Life Technologies, Breda, The Netherlands) by mixing 2 μg total RNA with 0.5 μg of oligo$(dT)_{12\text{-}18}$ primer in a total volume of 10 μl. After the mixture was heated at 70°C for 10 min, a solution containing 50 mM Tris·HCl (pH 8.3), 75 mM KCl, 3 mM $MgCl_2$, 10 mM DTT, 0.5 mM dNTPs, 0.5 μl RNase inhibitor, and 200 units of Superscript Reverse Transcriptase was added, resulting in a total volume of 20.5 μl. This mixture was incubated at 42°C for 1 h; total volume was adjusted to 100 μl with RNase-free water and stored at −80°C until further use. For real-time

quantitative PCR, 1 μl of first-strand cDNA diluted 1:10 in RNase-free water was used in a total volume of 25 μl, containing 12.5 μl 2X SYBR Green PCR Master Mix (Applied Biosystems) and 200 ng of each primer. Primers, designed with the Primer Express software package (Applied Biosystems), are listed in Table 1. PCR reactions, consisting of 95°C for 10 min (1 cycle), 94°C for 15 s, and 60°C for 1 min (40 cycles), were performed on an ABI Prism 7700 sequence detection system (Applied Biosystems). Data were analyzed with the ABI Prism 7700 sequence detection system version 1.9 software and quantified with the comparative threshold cycle method with β-actin as a housekeeping gene reference (31).

Protein assay. Total protein concentration was measured in bronchoalveolar lavage fluid (BALF) using the Dc protein assay (Bio-Rad), according to the manufacturer's instructions, with bovine serum albumin, fraction V (Roche Diagnostics, Mannheim, Germany) as a standard. The detection limit was 31 μg/ml.

Statistical analysis. Values are expressed as mean ± SE. Differences between groups were analyzed with ANOVA, followed by the Tukey multiple comparison test. For comparison of survival curves, Kaplan-Meier analysis followed by a log rank test was performed. Differences at P values of <0.05 were considered statistically significant.

Gene Product	Primers
	Forward primers
Amphiregulin	5′-TTTCGCTGGCGCTCTCA-3′
CINC-1	5′-GGGTGTCCCCAAGTAATGGA-3′
FGFR-4	5′-GTTGGCACGCAGCTCCTT-3′
Fra-1	5′-TTCTCCAGGACCCGTACTTGA-3′
IL-6	5′-ATATGTTCTCAGGGAGATCTTGGAA-3′
MCP-1	5′-TGGCAAGATGATCCCAATGA-3′
Met-1	5′-ATGTGCCCAGGGCTGTGT-3′
p21	5′-CATGTCCGATCCTGGTGATG-3′
PAI-1	5′-AGCTGGGCATGACTGACATCT-3′
TF	5′-CCCAGAAAGCATCACCAAGTC-3′
Upa	5′-ACAGCCATCCAGGACCATACA-3′
uPAR	5′-TGCTGGGAAACCGGAGTTAC-3′
β-actin	5′-TTCAACACCCCAGCCATGT-3′
	Reverse primers
Amphiregulin	5′-TTCCAACCCAGCTGCATAATG-3′
CINC-1	5′-CAGAAGCCAGCGTTCACCA-3′
FGFR-4	5′-GCAGGACCTTGTCCAGAGCTT-3′
Fra-1	5′-TCAGAGAGGGTGTGGTCATGAG-3′
IL-6	5′-TGCATCATCGCTGTTCATACAA-3′
MCP-1	5′-AGCTTCTTTGGGACACCTGCT-3′
Met-1	5′-GCAGCACTGTTCGTCACTTCA-3′
p21	5′-CGAACAGACGACGGCATACTT-3′
PAI-1	5′-GCTGCTCTTGGTCGGAAAGA-3′
TF	5′-TGCTCCACAATGATGAGTGTT-3′
uPA	5′-CCAAACGGAGCATCACCAA-3′
Upar	5′-GGAACCTTGGCACCAGGAA-3′
β-actin	5′-AGTGGTACGACCAGAGGCATACA-3′

Table 1. Sequences of oligonucleotides used as forward and reverse primers for real-time RT-PCR. [CINC-1, chemokine-induced neurtrophilic chemoattractant-1; FGFR-4, fibroblast growth factor receptor-4; MCP-1, monocyte chemoattractant protein-1; Met-1, methallothionein-1; PAI-1, plasminogen activator inhibitor-1; TF, tissue factor; uPA, urokinase-type plasminogen activator; uPAR, uPA receptor.]

RESULTS

Fibrin deposition. Because fibrin deposition is a sensitive marker for the severity of tissue damage in hyperoxia-induced lung injury, we quantified fibrin deposition in lung homogenates by Western blot analysis using the monoclonal 59D8 antibody against the 56-kDa fibrin β-chain. Fibrin deposition was quantified after exposure to two different NO concentrations (8.5 and 17 ppm) for 10 days to determine the optimal NO concentration to reduce hyperoxia-induced lung tissue damage (Figure 1*A*). Fibrin deposition was at background levels during normal neonatal pulmonary development in room air-exposed controls on *day 10* (19.9 ± 3.5 ng fibrin/mg tissue; Figure 1*B*). Fibrin deposition increased 19-fold to 382.5 ± 28.1 ng fibrin/tissue in

lungs of pups exposed to 100% oxygen for 10 days ($p < 0.001$). Continuous exposure to NO and 100% oxygen attenuated fibrin deposition 1.6-fold ($p < 0.01$) and 4.3-fold ($p < 0.001$) for 8.5 and 17 ppm NO, respectively. These results demonstrate that NO reduces fibrin deposition in a dosage-dependent way in experimental BPD, with 17 ppm NO as the most optimal concentration. In paraffin sections, extravascular fibrin deposits were detected in septae and alveoli after exposure to hyperoxia (Figure 1*D*), but were minor or even absent in 17 ppm NO-O_2 treated pups (Figure 1*E*). Pulmonary fibrin deposition was absent in normoxia (Figure 1*C*).

Since NO reduced fibrin deposition, a sensitive marker for lung tissue damage, in a dosage-dependent way, we only performed additional experiments, including immunohistology, survival, and capillary-alveolar leakage, with the most effective dosage of 17 ppm. Because quantitative RT-PCR and fibrin deposition could be determined in the same experimental pups, we included both NO dosages, 17 and 8.5 ppm, in our real-time RT-PCR studies.

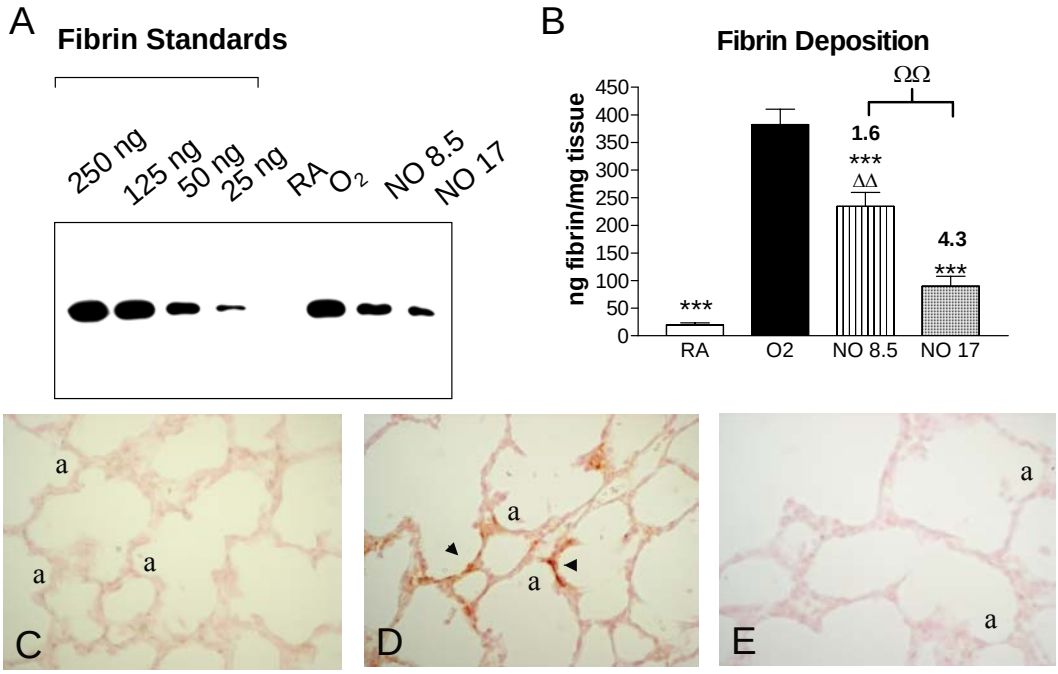

Figure 1. Western blot analysis of fibrin deposition, using monoclonal anti-human fibrin antibody 59D8, which specifically detects rat β-fibrin, in lung homogenates of rat pups exposed to room air (RA), oxygen (O_2), and O_2 in combination with 8.5 or 17 ppm nitric oxide (NO) for 10 days (*A*). Fibrin standards were used to quantify fibrin deposition. *B*: quantification of fibrin deposition in lung homogenates on *day 10*. Experimental groups include RA-exposed controls ($n = 10$), age-matched O_2-exposed controls ($n = 10$), and NO-treated O_2-exposed preterm rat pups with 8.5 ppm ($n = 10$) or 17 ppm NO ($n = 10$). Data are expressed as means ± SE of at least 10 rat pups. The number above the NO bars indicates the fold-difference in fibrin deposition between age-matched O_2-exposed controls and NO-O_2-exposed pups. ***$p < 0.001$ vs. age-matched O_2-exposed controls; $^{\Delta\Delta}p < 0.01$ vs. RA-exposed pups; $^{\Omega\Omega}p < 0.01$ for 8.5 vs. 17 ppm NO. Paraffin lung sections, stained with monoclonal 59D8, of RA-exposed controls (*C*), age-matched O_2-exposed controls (*D*), and NO-O_2 (17 ppm) rat pups (*E*) on *day 10*. Images are taken X400 magnification. Arrowheads in panel D indicate fibrin deposits in the alveolus of the lung. a, alveolus.

Growth and survival. At birth, *postnatal day 1*, mean body weight of the preterm rat pups was 4.9 g (Figure 2*A*). Growth of both oxygen (O_2)- and NO-O_2-exposed pups was similar until *day 10* when they weighed ~16 g. After *day 10*, mean body weight of the 17-ppm NO-O_2-exposed pups continued to increase until death. Survival of 17-ppm NO-O_2-exposed pups was prolonged compared to O_2-exposed controls (Figure 2*B*; $p < 0.001$). After 12 days of oxygen exposure, 95% of the controls had died vs. only 35% of the NO-O_2 pups. Median survival of O_2 controls and NO-O_2 pups was 11.5 and 13.0 days, respectively. A beneficial effect of 17-ppm NO-O_2 treatment on survival was observed after 10 days of oxygen exposure. Room air-exposed pups did not show signs of illness, and all survived the first 4 wk after birth (data not shown).

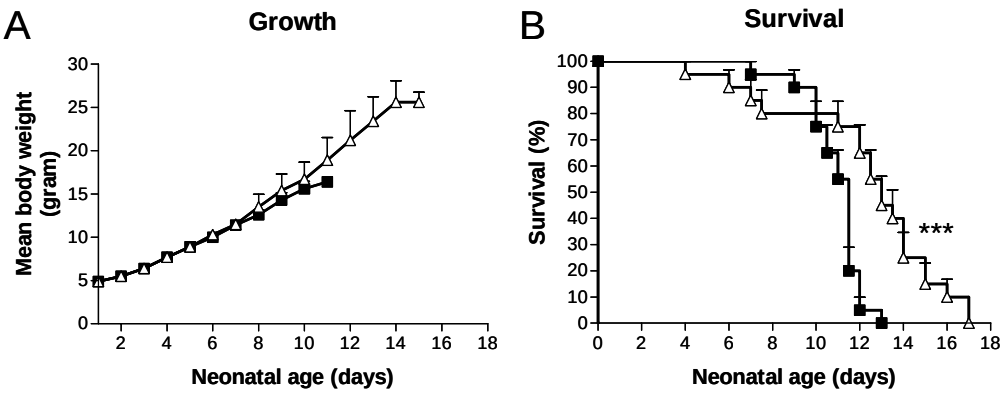

Figure 2. Growth in 17 ppm NO treated O_2 (NO-O_2)-exposed rat pups (Δ, $n = 20$) and age-matched O_2-exposed controls (■, $n = 20$) during the first 15 days after birth. Data are expressed as means ± SE (*A*). Kaplan-Meier survival curve of NO-O_2-exposed rat pups (Δ, $n = 20$) and age-matched O_2-exposed controls (■, $n = 20$) during the first 17 days after birth (*B*). Data are expressed as percentage ± SE of pups surviving at the observed time point (*B*). ***$p < 0.001$ for NO-O_2-exposed pups vs. age-matched O_2-exposed controls.

Lung histology. Preterm rats are born at the saccular stage of lung development. Sacculi are transformed into alveoli within 2 wk after birth by septal thinning and secondary septation. On *day 10*, alveoli are clearly visible during normal development (Figure 3*A*). Oxygen exposure for 10 days resulted in lung edema and a heterogeneous distribution of enlarged air-spaces, surrounded by septae with a marked increase in thickness (Figure 3*B*). After exposure to hyperoxia, the Lm (Figure 3*D*) increased by 33% ($p < 0.01$), and the alveolar surface area decreased 1.3-fold ($p < 0.001$) compared with room air-exposed controls (Figure 3*E*). iNO improved lung histopathology during hyperoxia exposure by reducing the influx of inflammatory cells and edema, thereby reducing septal thickness. Since iNO exposure improved secondary septation only marginally, iNO therapy resulted in enlarged alveoli that were surrounded by very thin septa (Figure 3*C*). This latter conclusion is in line with the observed 1.3-fold increase in alveolar surface area ($p < 0.001$) by iNO and the absence of a significant improvement of iNO on Lm, an indicator of mean alveolar diameter, which

only showed a tendency towards lower values after iNO treatment compared to hyperoxia-exposed pups. Hyperoxia led to a massive inflammatory reaction, characterized by an overwhelming influx of inflammatory cells (Figure 3*B*), including macrophages and neutrophilic granulocytes, compared to room air-exposed controls (Figure 3*A*).

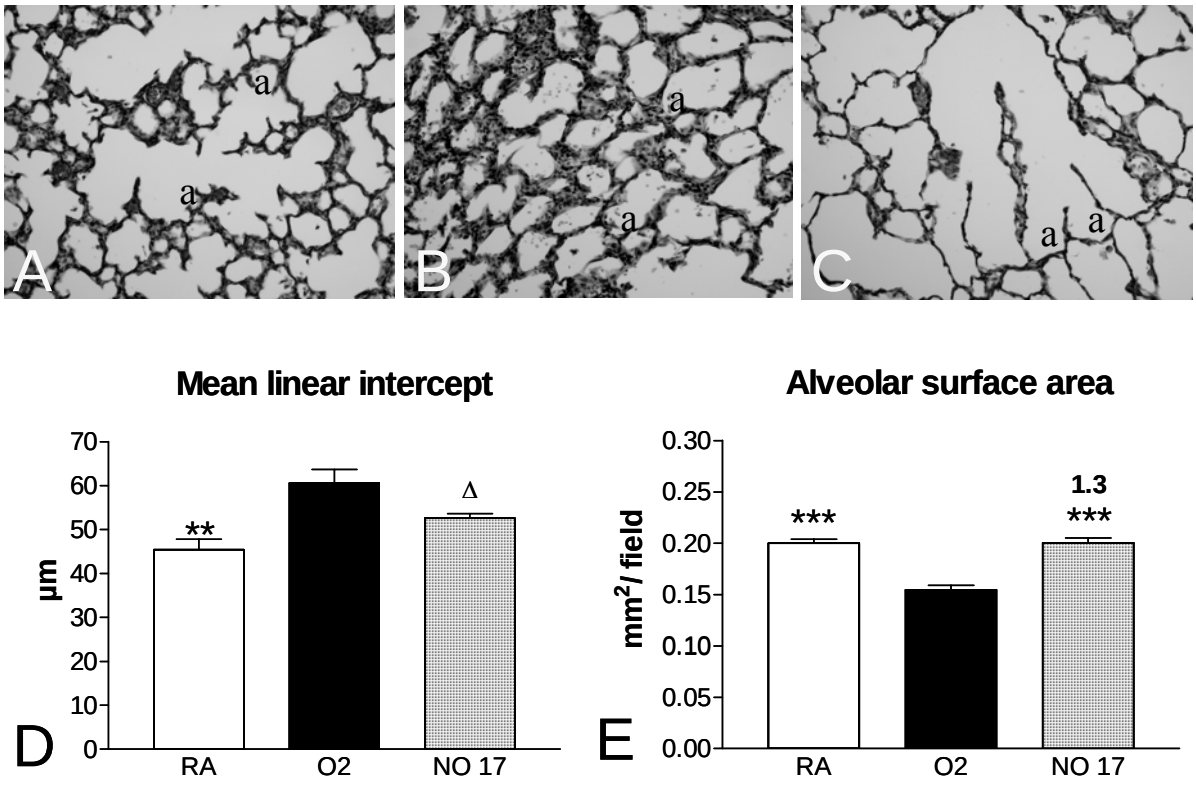

Figure 3. Paraffin lung sections stained with hematoxylin- and eosin of RA (*A*) and O_2-exposed controls (*B*) and age-matched 17 ppm NO-O_2-exposed pups (*C*) at 10 days of age. Images are X200 magnification. The mean linear intercept (*D*) and the alveolar surface area (*E*) were determined on paraffin sections in RA-exposed littermates, O_2-exposed rat pups, and 17 ppm NO-O_2-exposed pups. Note the presence of enlarged alveoli in *B* and *C* and thickened septae in *B*, which are significantly decreased after NO-O_2 treatment (*C*). Values are means $\pm$ SE in at least 6 different rat pups/group. a, alveolus. $^{**}p < 0.01$ and $^{***}p < 0.001$ vs. age-matched O_2-exposed controls; $^{\Delta}p < 0.05$ vs. RA-exposed rat pups.

Macrophages were detected with monoclonal ED-1 (Figure 4, *A*-*C*) and quantified by morphometry (Figure 4*D*). In control lungs (Figure 4*A*), resident ED-1-positive monocytes and macrophages were present at 250 cells/mm^2, which increased 16.4-fold ($p < 0.001$) in lungs of oxygen-exposed pups (Figure 4*B*). iNO (17 ppm NO-O_2 treatment) reduced the influx of ED-1-positive cells 3.4-fold ($p < 0.01$) compared with oxygen-exposed controls (Figure 4*C*), to levels that were not different from room air-exposed controls.

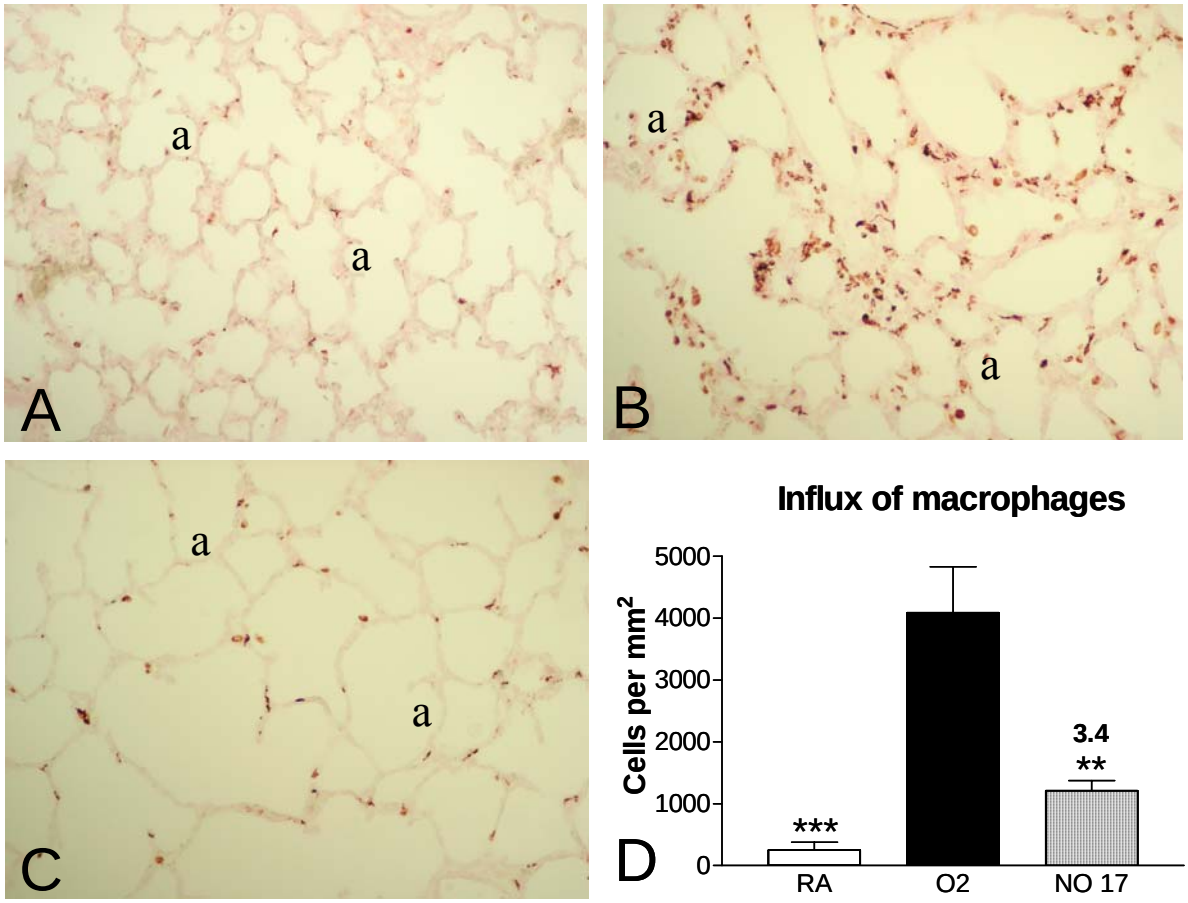

Figure 4. Paraffin lung sections stained with monoclonal ED-1 of RA (*A*) and O_2-exposed controls (*B*) and age-matched 17 ppm NO-O_2-exposed pups (*C*) at 10 days of age. Images are X200 magnification. Quantification of ED-1 positive monocytes and macrophages (*D*) was performed on paraffin sections in RA-exposed littermates, oxygen-exposed rat pups, and 17 ppm NO-O_2-exposed pups. Note the presence of large numbers of leukocytes, including neutrophils and macrophages in thickened septae and in the enlarged alveolar lumen, in *B*, which are significantly decreased after NO-O_2 treatment (*C*). Values are depicted as means ± SE in at least 6 different rat pups/group. a, alveolus. $^{**}p < 0.01$ and $^{***}p < 0.001$ vs. age-matched O_2-exposed controls.

Protein in BALF. To establish the inhibitory effect of iNO treatment on pulmonary edema by capillary-alveolar leakage in experimental BPD, total protein concentration was measured in BALF (Figure 5). Protein concentration on *postnatal day 10* was 65 ± 12 µg/ml in room air-exposed pups, 410 ± 60 µg/ml in oxygen-exposed controls, and 213 ± 22 µg/ml in 17 ppm NO-O_2 treated pups ($p < 0.01$ vs. oxygen-exposed controls).

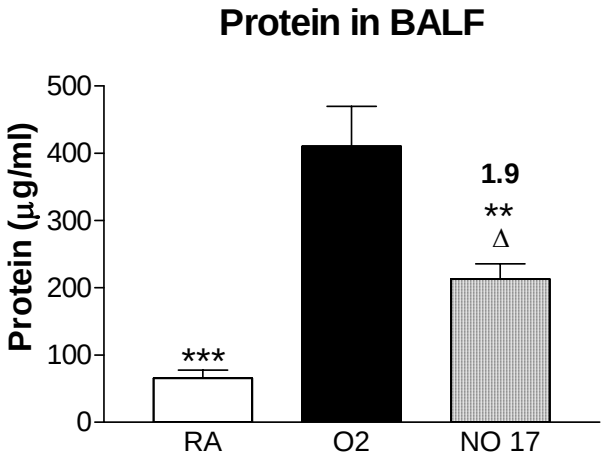

Figure 5. Total protein concentration in bronchoalveolar lavage fluid (BALF) of RA-exposed controls, age-matched O_2-exposed controls, and 17 ppm NO-O_2 treated rat pups on *day 10*. Data are expressed as means ± SE of 6 rats/group. $^{**}p < 0.01$ and $^{***}p < 0.001$ vs. age-matched O_2-exposed controls. $^{\Delta}p < 0.05$ vs. RA-exposed rat pups.

mRNA expression in lung homogenates. Hyperoxia-induced lung injury induces alterations in inflammation, coagulation, fibrinolysis, fibrosis, extracellular matrix turnover, alveolar enlargement, edema, cell cycle, gas exchange and oxidative stress response. Therefore, we studied differential expression of key genes of these pathways, previously characterized in this rat model for experimental BPD (41), with real-time RT-PCR in lungs of pups exposed to room air, 100% oxygen, or 100% oxygen with 8.5 or 17 ppm NO (NO-O_2) on *postnatal day 10* to characterize the optimal NO response in hyperoxia-induced lung injury.

Inflammation. Ten days of oxygen exposure resulted in an increase in mRNA expression of the proinflammatory cytokine IL-6 (178-fold; $p < 0.001$), the chemokines chemokine-induced neutrophilic chemoattractant-1 (CINC-1, 7.0-fold; $p < 0.001$) and monocyte chemoattractant protein-1 (MCP-1, 10.4-fold; $p < 0.001$), and the growth factor amphiregulin (4.2-fold; $p < 0.001$) in lungs of oxygen-exposed pups compared to room air-exposed controls (Figure 6). Exposure of pups to 8.5 ppm NO-O_2 decreased mRNA expression 3.0-fold ($p = 0.02$; Figure 6*A*) for IL-6, 1.8-fold ($p < 0.01$; Figure 6*B*) for CINC-1 and 2.9-fold for amphiregulin ($p < 0.001$) compared with hyperoxia-exposed controls. Expression of the other inflammatory genes was not altered after 8.5 ppm NO-O_2 treatment. In pups treated with 17 ppm NO-O_2, the decrease in mRNA expression of the inflammatory genes was more pronounced: 4.9-fold for IL-6 ($p < 0.001$; Figure 6*A*) and 2.1-fold for CINC-1 ($p < 0.001$; Figure 6*B*).

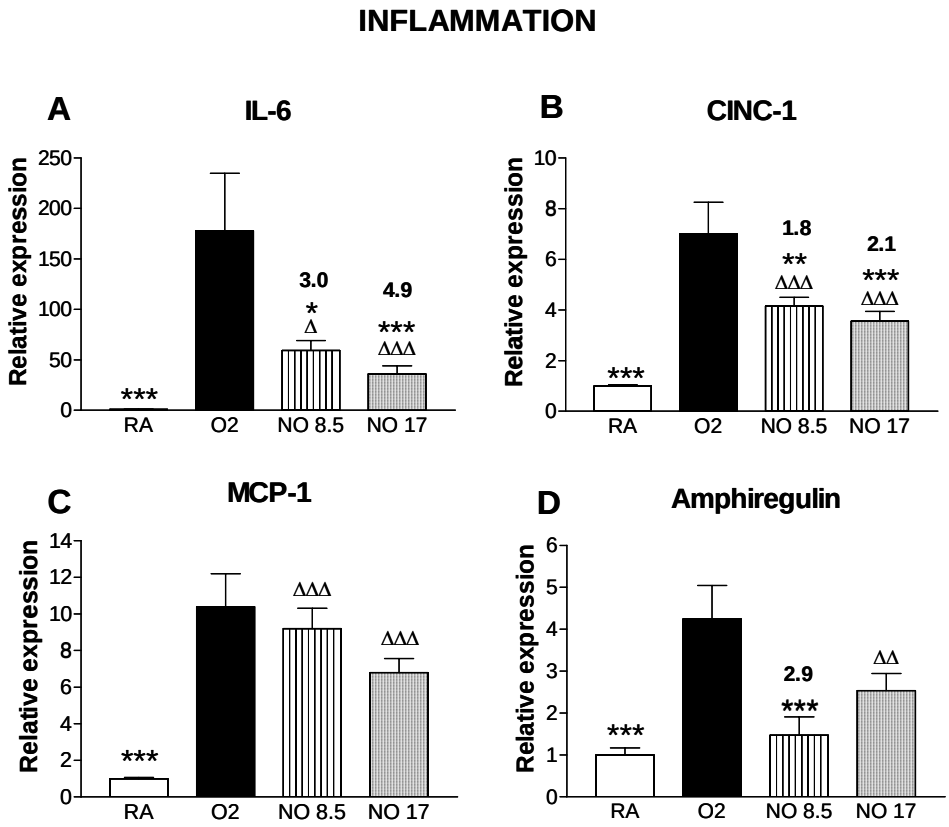

Figure 6. Relative mRNA expression, determined with RT-PCR, of genes related to inflammation: IL-6 (*A*), chemokine-induced neutrophilic chemoattractant-1 (CINC-1; *B*), monocyte chemoattractant protein-1 (MCP-1; *C*), and amphiregulin (*D*) in RA-exposed controls, age-matched O_2-exposed controls, and NO-treated oxygen-exposed rat pups with 8.5 ppm or 17 ppm on *day 10*. Data are expressed as means ± SE of at least 10 rat pups. The number above the NO bars indicates the fold-difference in relative expression between age-matched O_2-exposed controls and NO-O_2-exposed pups. *$p < 0.05$, **$p < 0.01$, and ***$p < 0.001$ vs. age-matched O_2-exposed controls. $^{\Delta}p < 0.05$, $^{\Delta\Delta}p < 0.01$, and $^{\Delta\Delta\Delta}p < 0.001$ vs. RA-exposed rat pups.

Coagulation and fibrinolysis. Oxygen exposure resulted in an upregulation of pulmonary mRNA expression of the procoagulant factor tissue factor (TF, 5.0-fold; $p < 0.001$) and the fibrinolytic factors plasminogen activator inhibitor-1 (PAI-1, 29-fold; $p < 0.001$), urokinase-type plasminogen activator (uPA, 1.7-fold; $p < 0.001$) and urokinase-type plasminogen activator receptor (uPAR, 4.1-fold, $p < 0.001$) on *day 10* compared with room air-exposed controls (Figure 7). Exposure to 8.5 ppm NO-O_2 resulted in a 1.7-fold reduction of PAI-1 ($p < 0.01$; Figure 7B) and a 1.4-fold reduction of uPAR ($p = 0.02$; Figure 7D), whereas 17 ppm NO-O_2 treatment only resulted in a 1.5-fold reduction of PAI-1 ($p = 0.02$; Figure 7B) compared with oxygen-exposed controls. TF and uPA mRNA expression was not significantly affected by iNO (Figure 7A and 7C).

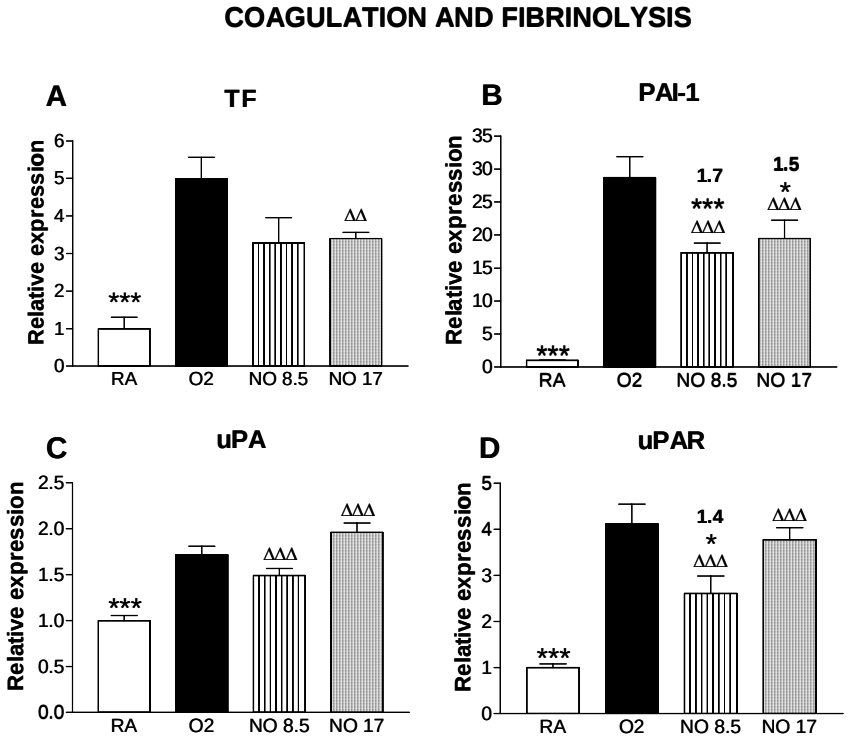

Figure 7. Relative mRNA expression, determined with RT-PCR, of genes related to coagulation and fibrinolysis: tissue factor (TF; *A*), plasminogen activator inhibitor-1 (PAI-1; *B*), urokinase-type plasminogen activator (uPA; *C*), and urokinase-type plasminogen activater receptor (uPAR; *D*) in RA-exposed controls, age-matched O_2-exposed controls, and NO-treated O_2-exposed rat pups with 8.5 ppm or 17 ppm on *day 10*. Data are expressed as means ± SE of at least 10 rat pups. The number above the NO bars indicates the fold-difference in relative expression between age-matched O_2-exposed controls and NO-O_2-exposed pups. *p < 0.05 and ***p < 0.001 vs. age-matched O_2-exposed controls. $^{\Delta\Delta}p$ < 0.01 and $^{\Delta\Delta\Delta}p$ < 0.001 vs. RA-exposed rat pups.

Alveolar enlargement, cell-cycle, signal transduction and anti-oxidants. mRNA expression of fibroblast growth factor receptor-4 (FGFR-4), a membrane receptor involved in secondary septation and alveolar enlargement, was decreased in lungs of oxygen-exposed pups compared with room air-exposed controls (7.6-fold; p < 0.001; Figure 8*A*). Exposure to 17 ppm NO, but not 8.5 ppm, significantly upregulated the expression of FGFR-4, 1.8-fold (p < 0.001; Figure 8*A*) compared with oxygen-exposed controls. Hyperoxia upregulated pulmonary mRNA expression of the cell cycle inhibitor cyclin-dependent kinase inhibitor p21 (14.4-fold; p < 0.001; Figure 8*B*) and the antioxidant methallothionein-1 (Met-1, 2.6-fold, p = 0.004; Figure 8*D*) compared with room air-exposed controls, whereas expression of activator protein-1 (AP-1) gene fos-related antigen-1, which plays a role in signal transduction, was not significantly altered (Figure 8*C*). Treatment with NO-O_2 only resulted in a 1.3-fold and 1.4-fold (p < 0.01; Figure 8*B*) reduction in p21 mRNA expression after exposure to 8.5 and 17 ppm NO-O_2, respectively, whereas Fra1 and Met-1 mRNA expression was not significantly changed, compared with oxygen-exposed controls (Figure 8*C* and 8*D*). Fra1 mRNA expression was 2.5 fold (p < 0.05; Figure 8*C*) decreased after exposure to 17 ppm NO-O_2 compared with 8.5 ppm NO-O_2.

ALVEOLAR ENLARGEMENT, CELL-CYCLE, SIGNAL TRANSDUCTION AND ANTI-OXIDANTS

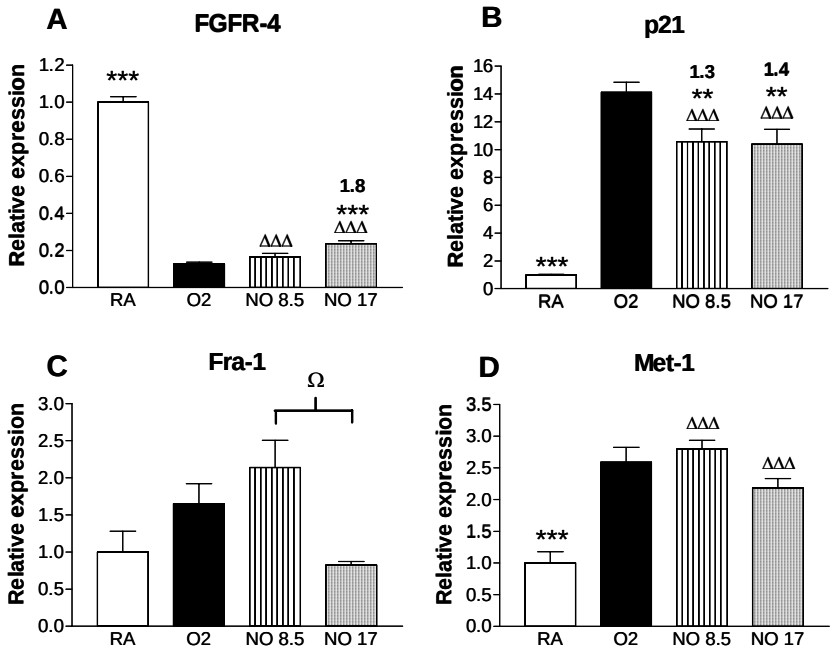

Figure 8. Relative mRNA expression, determined with RT-PCR, of genes related to alveolar enlargement: fibroblast growth facter receptor-4 (FGFR4; *A*), cell-cycle (p21; *B*), signal transduction (Fra-1; *C*), and the antioxidant methallothionein-1 (Met-1; *D*) in RA-exposed controls, age-matched O_2-exposed controls, and NO-treated O_2-exposed rat pups with 8.5 ppm or 17 ppm on *day 10*. Data are expressed as means ± SE of at least 10 rat pups. The number above the NO bars indicates the fold-difference in relative expression between age-matched O_2-exposed controls and NO-O_2-exposed pups. $^{**}p < 0.01$, and $^{***}p < 0.001$ vs. age-matched O_2-exposed controls. $^{\Delta\Delta\Delta}p < 0.001$ versus RA-exposed rat pups. $^{\Omega}p < 0.05$ for 8.5 vs. 17 ppm NO.

DISCUSSION

iNO therapy markedly improves lung pathology and prolongs survival by inhibiting inflammation and reducing capillary-alveolar protein leakage and alveolar fibrin deposition in premature rat pups exposed to prolonged hyperoxia, a chronic lung injury model that closely resembles BPD in premature infants (41).

Inhibition of inflammation was demonstrated by a reduction in the expression of the proinflammatory factor IL-6, MCP-1, CINC-1 and the growth factor amphiregulin. This observation was supported by histopathological findings, such as a reduced influx of leukocytes, including a 3.4-fold decrease in ED-1-positive monocytes and macrophages, and neutrophilic granulocytes and less edema as suggested by a twofold reduction in capillary-alveolar leakage, assuming that edema protein levels are not affected by differences in Na^+ channel-dependent alveolar fluid clearance by the alveolar epithelial cells in iNO-treated pups and hyperoxia-

exposed controls. These pathological findings are in agreement with observations in premature lambs exposed to 20 ppm of iNO (21) but contradict histopathological findings in adult rats exposed to 100 ppm of iNO (30). However, an iNO dosage of 100 ppm may be too toxic to attenuate hyperoxia-induced lung neutrophil accumulation, since NO is a highly reactive free radical with significant toxic potential (43). A protective role of endogenous NO production has been suggested by a study in transgenic mice lacking iNOS in which hyperoxia-induced lung injury is greater than in wild-type mice (24). In contrast, in another study using iNOS deficient mice, the injurious response to intratracheal administration of bleomycin was attenuated (9). Collectively, these studies confirm the important, but divergent, role of NO in experimental inflammatory lung diseases. We recently reported the proinflammatory role of IL-6, CINC-1, and amphiregulin in neonatal hyperoxia-induced lung injury (41). The current data confirm that a reduction of these proinflammatory factors with iNO inhibits the development of experimental BPD.

Fibrin deposition is an important contributor to the pathogenesis of lung injury by oxidative stress. In both human and animal lung injury, intra-alveolar and intravascular fibrin deposition is correlated with a poorer prognosis (3, 37). We detected a significant NO-induced reduction of fibrin deposition that was at least partially confirmed at the transcriptional level by reduced PAI-1 expression, a tendency towards lower TF expression, and reduced capillary-alveolar leakage after NO treatment. In experimental BPD, pulmonary fibrin deposits are primarily localized in the extravascular compartment alveolar lumen and associated with the alveolar inner membrane (37). The extravascular localization of fibrin suggests capillary-alveolar leakage of plasma proteins, including fibrinogen, into the alveolar lumen followed by local conversion into fibrin by thrombin. The reduction of fibrin and the attenuation of TF and/or PAI-1 expression seem to contribute to a better outcome in experimental BPD (this study, 4, 37). Fibrin may induce lung injury in various ways. It exerts proinflammatory and profibrotic properties by facilitating cell migration and activating inflammatory cells and fibroblasts, probably via the activation of NF-κB and AP-1 (35), and can hamper pulmonary gas exchange via inactivation of lung surfactant (11). The data suggest that reduced capillary leakage or transcriptional regulation of the fibrinolytic cascade by PAI-1, rather than the coagulation cascade by TF, plays an important role in reducing fibrin deposition by NO in experimental BPD.

The anti-inflammatory and anticoagulant effects of NO can also be attributed to inhibition of the redox-responsive transcription factor NF-κB, observed previously in adult rats (16) and transgenic mice (15) with lung injury. Because expression of IL-6, CINC-1, and TF is regulated at a transcriptional level by NF-κB and/or AP-1 (32), inhibition of NF-κB and/or AP-1 by NO can indirectly lead to attenuation of pulmonary inflammation and coagulation in lung injury. Since AP-1 and NF-κB are also involved in the expression of p21 and Fra-1, genes related to cell cycle and signal transduction (32), reduced expression of both cell cycle proteins by iNO during hyperoxia can at least in part be explained by inhibition of AP-1 and

NF-κB.

As NO is a free radical and hyperoxia increases the production of oxygen radicals, we expected an effect on the antioxidant Met-1 during oxygen and NO exposure. Hyperoxia increased the expression of Met-1, but additional NO-treatment did not change the expression of Met-1. In contrast, Turanlahti et al. (39) demonstrated that hyperoxia and 40 ppm of NO each induced free radical-mediated lung injury, whereas the combination of hyperoxia and NO significantly attenuated pulmonary free radical-mediated effects. The higher NO dosage used in Turanlahti's experiments possibly might explain the discrepancy between both studies.

Prolonged oxidative stress arrests alveolar development in premature infants. Histology is characterized by irregularly shaped, enlarged saccular-like air spaces, surrounded by thickened septae. iNO-treatment markedly improves lung pathology by reducing septal thickness and increasing alveolar surface area in our experimental BPD model, but alveolarization is still disturbed, probably due to impaired secondary septation as demonstrated by the absence of a significant improvement of the mean linear intercept. This improved lung pathology confirms the results obtained in premature baboons developing BPD, in whom lung growth and pulmonary function improved and elastin deposition decreased after prolonged exposure to low dose (5 ppm) iNO (27). Impaired alveolarization suggests partial but not sufficient improvement of iNO-mediated mRNA expression of the cell cycle inhibitor p21 and FGFR-4 and is in agreement with observations in FGFR-3(-/-)/FGFR-4(-/-) mice. Lungs of FGFR-3(-/-)/FGFR-4 (-/-) mice are normal at birth but have a complete block in alveogenesis and do not form secondary septae, demonstrating a cooperative function of FGFR-4 to promote the formation of alveoli (44).

Survival of hyperoxia-exposed premature rat pups was significantly prolonged by iNO therapy. Median survival was 1.5 days longer in premature rat pups treated with 17 ppm iNO and oxygen than in oxygen-exposed controls. Other animal studies of neonatal hyperoxic lung injury did not focus on survival (6, 18, 21, 25, 27, 34), but iNO prolongs survival in adult rats with hyperoxia-induced lung injury (12, 30). Nelin et al. (30) exposed rats to hyperoxia for 120 h and either 10 or 100 ppm iNO. Rats treated with 100 ppm iNO had an increased survival, but rats treated with 10 ppm iNO did not. Gutierrez et al. (12) reported prolonged survival in adult rats exposed to hyperoxia and low-dose iNO (5-10 ppm). Rat pups have a greater tolerance to hyperoxia than adult rats, and lung injury induced by hyperoxia in rat pups closely resembles chronic lung injury or BPD in premature infants. Only one clinical iNO trial has shown both an improved survival and a lower incidence of BPD in premature infants randomized to iNO vs. placebo (33). Premature infants treated with iNO also had a better neurodevelopmental outcome at follow-up at 2 years of age (29). However, this study is an exception because other clinical trials did not detect a positive effect of iNO therapy on survival (2, 5, 14, 22, 23, 40), despite an improvement in oxygenation (14, 22), or on prevention of BPD in premature infants. Kinsella et al. (23) and Ballard et al. (2) recently reported on two large trials of iNO in premature infants. In the trial by Kinsella et al (23), starting with 5 ppm

of iNO soon after birth did not reduce death or BPD, but reduced the incidence of brain injury detected by cranial ultrasound (23). In the trial by Ballard et al. (2), an initial dose of 20 ppm iNO for 2-4 days followed by weekly halving of the dose improved survival without BPD in infants who were 7-14 days of age at randomization, but did not reduce the incidence of brain injury. These reports suggest a possible benefit of iNO, but clinical use of iNO in ventilated premature infants awaits more data on dosing, duration, time of initiation, and long-term follow-up (36). Higher NO dosages may further improve outcome, despite the lingering fears of adverse effects of NO treatment, such as brain injury, enterocolitis, or patent ductus arteriosus, which have not materialized in low-dose studies (14, 22, 33, 40).

In summary, this study demonstrates that iNO therapy improves lung pathology and prolongs survival in premature rat pups with experimental BPD by inhibiting inflammation and capillary- alveolar leakage and reducing alveolar fibrin deposition with 17 ppm NO as most effective dosage with the least side effects. iNO has considerable potential towards improving pulmonary function and outcome in ventilated premature infants.

ACKNOWLEDGMENTS

We thank E. de Boer, M.A. van Gastelen and S. Sengupta for expert technical assistance. Dr. J.C.M. Meijers kindly provided 59D8 antibody, and ED-1 antibody was a gift from Dr. E. de Heer.

GRANTS

This study was supported by Grant 920-03-213 from The Netherlands Organization for Health Research and Development (S. A. J. ter Horst), a grant from the Stichting Prof. A. H. H. Kassenaar Fonds (G. T. M. Wagenaar and F. J. Walther), a grant from the Gisela Thier fund (F. J. Walther) and National Heart, Lung, and Blood Institute Grant HL-55534 (F. J. Walther).

REFERENCES

1. **Balasubramaniam V, Tang JR, Maxey A, Plopper CG and Abman SH.** Mild hypoxia impairs alveolarization in the endothelial nitric oxide synthase-deficient mouse. *Am J Physiol Lung Cell Mol Physiol* 284: L964-L971, 2003.
2. **Ballard RA, Truog WE, Cnaan A, Martin RJ, Ballard PL, Merrill JD, Walsh MC, Durand DJ, Mayock DE, Eichenwald EC, Null DR, Hudak ML, Puri AR, Golombek SG, Courtney SE, Stewart DL, Welty SE, Phibbs RH, Hibbs AM, Luan X, Wadlinger SR, Asselin JM and Coburn CE.** Inhaled nitric oxide in preterm infants undergoing mechanical ventilation. *N Engl J Med* 355: 354-364, 2006.
3. **Barazzone C, Belin D, Piguet PF, Vassalli JD and Sappino AP.** Plasminogen activator inhibitor-1 in acute hyperoxic mouse lung injury. *J Clin Invest* 98: 2666-2673, 1996.
4. **Carraway MS, Welty-Wolf KE, Miller DL, Ortel TL, Idell S, Ghio AJ, Petersen LC and Piantadosi CA.** Blockade of tissue factor: treatment for organ injury in established sepsis. *Am J Respir Crit Care Med* 167: 1200-1209, 2003.
5. **Clark RH, Kueser TJ, Walker MW, Southgate WM, Huckaby JL, Perez JA, Roy BJ, Keszler M and Kinsella JP.** Low-dose nitric oxide therapy for persistent pulmonary hypertension of the newborn. Clinical Inhaled Nitric Oxide Research Group. *N Engl J Med* 342: 469-474, 2000.
6. **Cummings JJ.** Nitric oxide decreases lung liquid production in fetal lambs. *J Appl Physiol* 83: 1538-1544, 1997.
7. **Dijkstra CD, Dopp EA, Joling P and Kraal G.** The heterogeneity of mononuclear phagocytes in lymphoid organs: distinct macrophage subpopulations in the rat recognized by monoclonal antibodies ED1, ED2 and ED3. *Immunology* 54: 589-599, 1985.
8. **Gaston B, Drazen JM, Loscalzo J and Stamler JS.** The biology of nitrogen oxides in the airways. *Am J Respir Crit Care Med* 149**:** 538-551, 1994.
9. **Genovese T, Cuzzocrea S, Di Paola R, Failla M, Mazzon E, Sortino MA, Frasca G, Gili E, Crimi N, Caputi AP and Vancheri C.** Inhibition or knock out of inducible nitric oxide synthase result in resistance to bleomycin-induced lung injury. *Respir Res* 6: 58, 2005.
10. **Goodman G, Perkin RM, Anas NG, Sperling DR, Hicks DA and Rowen M.** Pulmonary hypertension in infants with bronchopulmonary dysplasia. *J Pediatr* 112**:** 67-72, 1988.
11. **Gupta M, Hernandez-Juviel JM, Waring AJ, Bruni R and Walther FJ.** Comparison of functional efficacy of surfactant protein B analogues in lavaged rats. *Eur Respir J.* 16: 1129-1133, 2000.
12. **Gutierrez HH, Nieves B, Chumley P, Rivera A and Freeman BA.** Nitric oxide regulation of superoxide-dependent lung injury: oxidant-protective actions of endogenously produced and exogenously administered nitric oxide. *Free Radic Biol Med* 21: 43-52, 1996.
13. **Hamon I, Fresson J, Nicolas MB, Buchweiller MC, Franck P and Hascoet JM.** Early inhaled nitric oxide improves oxidative balance in very preterm infants. *Pediatr Res.* 57: 637-643, 2005.
14. **Hascoet JM, Fresson J, Claris O, Hamon I, Lombet J, Liska A, Cantagrel S, Al Hosri J, Hiriez G, Valdes V, Vittu G, Egreteau L, Henrot A, Buchweiller MC and Onody P.** The safety and efficacy of nitric oxide therapy in premature infants. *J Pediatr* 146: 318-323, 2005.
15. **Hesse AK, Dorger M, Kupatt C and Krombach F.** Proinflammatory role of inducible nitric oxide synthase in acute hyperoxic lung injury. *Respir Res* 5: 11, 2004.
16. **Howlett CE, Hutchison JS, Veinot JP, Chiu A, Merchant P and Fliss H.** Inhaled nitric oxide protects against hyperoxia-induced apoptosis in rat lungs. *Am J Physiol* 277: L596-L605, 1999.
17. **Hui KY, Haber E and Matsueda GR.** Monoclonal antibodies to a synthetic fibrin-like peptide bind to human fibrin but not fibrinogen. *Science* 222: 1129-1132, 1983.

18. **Issa A, Lappalainen U, Kleinman M, Bry K and Hallman M.** Inhaled nitric oxide decreases hyperoxia-induced surfactant abnormality in preterm rabbits. *Pediatr Res* 45: 247-254, 1999.
19. **Jobe AH and Ikegami M.** Mechanisms initiating lung injury in the preterm. *Early Hum Dev* 53**:** 81-94, 1998.
20. **Kermarrec N, Zunic P, Beloucif S, Benessiano J, Drouet L and Payen D.** Impact of inhaled nitric oxide on platelet aggregation and fibrinolysis in rats with endotoxic lung injury. Role of cyclic guanosine 5'-monophosphate. *Am J Respir Crit Care Med* 158: 833-839, 1998.
21. **Kinsella JP, Parker TA, Galan H, Sheridan BC, Halbower AC and Abman SH.** Effects of inhaled nitric oxide on pulmonary edema and lung neutrophil accumulation in severe experimental hyaline membrane disease. *Pediatr Res* 41: 457-463, 1997.
22. **Kinsella JP, Walsh WF, Bose CL, Gerstmann DR, Labella JJ, Sardesai S, Walsh-Sukys MC, McCaffrey MJ, Cornfield DN, Bhutani VK, Cutter GR, Baier M and Abman SH.** Inhaled nitric oxide in premature neonates with severe hypoxaemic respiratory failure: a randomised controlled trial. *Lancet* 354: 1061-1065, 1999.
23. **Kinsella JP, Cutter GR, Walsh WF, Gerstmann DR, Bose CL, Hart C, Sekar KC, Auten RL, Bhutani VK, Gerdes JS, George TN, Southgate WM, Carriedo H, Couser RJ, Mammel MC, Hall DC, Pappagallo M, Sardesai S, Strain JD, Baier M and Abman SH.** Early inhaled nitric oxide therapy in premature newborns with respiratory failure. *N Engl J Med* 355: 354-364, 2006.
24. **Kobayashi H, Hataishi R, Mitsufuji H, Tanaka M, Jacobson M, Tomita T, Zapol WM and Jones RC.** Anti-inflammatory properties of inducible nitric oxide synthase in acute hyperoxic lung injury. *Am J Respir Cell Mol Biol.* 24**:** 390-397, 2001.
25. **Lin YJ, Markham NE, Balasubramaniam V, Tang JR, Maxey A, Kinsella JP and Abman SH.** Inhaled nitric oxide enhances distal lung growth after exposure to hyperoxia in neonatal rats. *Pediatr Res* 58**:** 22-29, 2005.
26. **de Magalhães Simões S, dos Santos MA, da Silva Oliveira M, Fontes ES, Fernezlian S, Garippo AL, Castro I, Castro FFM, de Arruda Martins M, Saldiva PHN, Mauad T and Dolhnikoff M.** Inflammotory cell mapping of the respiratory tract in fatal asthma. *Clin Exp Allergy* 35: 602-611, 2005.
27. **McCurnin DC, Pierce RA, Chang LY, Gibson LL, Osborne-Lawrence S, Yoder BA, Kerecman JD, Albertine KH, Winter VT, Coalson JJ, Crapo JD, Grubb PH and Shaul PW.** Inhaled NO improves early pulmonary function and modifies lung growth and elastin deposition in a baboon model of neonatal chronic lung disease. *Am J Physiol Lung Cell Mol Physiol* 288: L450-L459, 2005.
28. **McElroy MC, Wiener-Kronish JP, Miyazaki H, Sawa T, Modelska K, Dobbs LG and Pittet JF.** Nitric oxide attenuates lung endothelial injury caused by sublethal hyperoxia in rats. *Am J Physiol* 272: L631-L638, 1997.
29. **Mestan KK, Marks JD, Hecox K, Huo D and Schreiber MD.** Neurodevelopmental outcomes of premature infants treated with inhaled nitric oxide. *N Engl J Med* 353: 23-32, 2005.
30. **Nelin LD, Welty SE, Morrisey JF, Gotuaco C and Dawson CA.** Nitric oxide increases the survival of rats with a high oxygen exposure. *Pediatr Res* 43: 727-732, 1998.
31. **Pfaffl MW.** A new mathematical model for relative quantification in real-time RT-PCR. *Nucleic Acids Res* 29: e45, 2001.
32. **Roebuck KA, Carpenter LR, Lakshminarayanan V, Page SM, Moy JN and Thomas LL.** Stimulus-specific regulation of chemokine expression involves differential activation of the redox-responsive transcription factors AP-1 and NF-kappaB. *J Leukoc Biol* 65: 291-298, 1999.
33. **Schreiber MD, Gin-Mestan K, Marks JD, Huo D, Lee G and Srisuparp P.** Inhaled nitric oxide in premature infants with the respiratory distress syndrome. *N Engl J Med* 349: 2099-2107, 2003.
34. **Shaul PW, Afshar S, Gibson L L, Sherman TS, Kerecman JD, Grubb PH, Yoder BA and McCurnin DC.** Developmental changes in nitric oxide synthase isoform expression and nitric oxide production in fetal baboon lung. *Am J Physiol Lung Cell Mol*

Physiol 283**:** L1192-L1199, 2002.
35. **Sitrin RG, Pan PM, Srikanth S and Todd RF 3rd.** Fibrinogen activates NF-kappa B transcription factors in mononuclear phagocytes. *J Immunol* 161: 1462-1470, 1998.
36. **Stark AR.** Inhaled NO for preterm infants. Getting to yes? *N Engl J Med* 355: 404-406, 2006.
37. **ter Horst SAJ, Wagenaar GTM, de Boer E, van Gastelen MA, Meijers JCM, Biemond BJ, Poorthuis BJHM and Walther FJ.** Pentoxifylline reduces fibrin deposition and prolongs survival in neonatal hyperoxic lung injury. *J Appl Physiol* 97: 2014-2019, 2004.
38. **The Franco-Belgium Collaborative NO Trial Group.** Early compared with delayed inhaled nitric oxide in moderately hypoxaemic neonates with respiratory failure: a randomised controlled trial. *Lancet* 354: 1066-1071, 1999.
39. **Turanlahti M, Pesonen E, Lassus P and Andersson S.** Nitric oxide and hyperoxia in oxidative lung injury. *Acta Paediatr* 89: 966-970, 2000.
40. **van Meurs KP, Wright LL, Ehrenkranz RA, Lemons JA, Ball MB, Poole WK, Perritt R, Higgins RD, Oh W, Hudak ML, Laptook AR, Shankaran S, Finer NN, Carlo WA, Kennedy KA, Fridriksson JH, Steinhorn RH, Sokol GM, Konduri GG, Aschner JL, Stoll BJ, D'Angio CT and Stevenson DK.** Inhaled nitric oxide for premature infants with severe respiratory failure. *N Engl J Med* 353: 13-22, 2005.
41. **Wagenaar GTM, ter Horst SAJ, van Gastelen MA, Leijser LM, Mauad T, van der Velden PA, de Heer E, Hiemstra PS, Poorthuis BJHM and Walther FJ.** Gene expression profile and histopathology of experimental bronchopulmonary dysplasia induced by prolonged oxidative stress. *Free Radic Biol Med* 36: 782-801, 2004.
42. **Walther FJ, Benders MJ and Leighton JO.** Persistent pulmonary hypertension in premature neonates with severe respiratory distress syndrome. *Pediatrics* 90**:** 899-904, 1992.
43. **Warren JB and Higenbottam T.** Caution with use of inhaled nitric oxide. *Lancet* 348: 629-630, 1996.
44. **Weinstein M, Xu X, Ohyama K and Deng CX.** FGFR-3 and FGFR-4 function cooperatively to direct alveogenesis in the murine lung. *Development* 125: 3615-3623, 1998.